Inorganic Chemistry

Article

pubs.acs.org/IC

Spin Crossover in Tetranuclear Fe(II) Complexes, {[(tpma)Fe(μ-CN)]$_4$}X$_4$ (X = ClO_4^-, BF_4^-)

Oleksandr Hietsoi,[†,∥] Paul W. Dunk,[†,∥] Heather D. Stout,[‡] Alejandra Arroyave,[†] Kirill Kovnir,[†,⊥] Raechel E. Irons,[†] Nazira Kassenova,[§] Rakhmetulla Erkasov,[§] Catalina Achim,*[,‡] and Michael Shatruk*[,†]

[†]Department of Chemistry and Biochemistry, Florida State University, 95 Chieftan Way, Tallahassee, Florida 32306, United States

[‡]Department of Chemistry, Carnegie Mellon University, 4400 Fifth Avenue, Pittsburgh, Pennsylvania 15213, United States

[§]Department of Chemistry, L. N. Gumilyov Eurasian National University, 5 Munaitpasov Str., 010008 Astana, Kazakhstan

Supporting Information

ABSTRACT: Two Fe(II) complexes, {[(tpma)Fe(μ-CN)]$_4$}X$_4$ (X = ClO_4^- (**1a**), BF_4^- (**1b**); tpma = tris(2-pyridylmethyl)-amine), were prepared by reacting the {Fe(tpma)}$^{2+}$ building block with $(Bu_4N)CN$. The crystal structures of **1a** and **1b** feature a tetranuclear cation composed of cyanide-bridged Fe(II) ions, each capped with a tetradentate tpma ligand. The Fe$_4$(μ-CN)$_4$ core of the complex is strongly distorted, assuming a butterfly-like geometry. Both complexes exhibit gradual temperature-driven spin crossover (SCO) associated with the high-spin (HS) ↔ low-spin (LS) transition at two out of four metal centers. The evolution of HS and LS Fe(II) ions with temperature was followed by a combination of X-ray crystallography, magnetic measurements, and Mössbauer spectroscopy. Only the Fe(II) ions surrounded by six N atoms undergo the SCO. A comparison of the temperature-dependent SCO curves for the samples stored under solvent and the dried samples shows that the former exhibit a much more abrupt SCO. This finding was interpreted in terms of the increased structural disorder and decreased crystallinity caused by the loss of the interstitial solvent molecules in the dried samples.

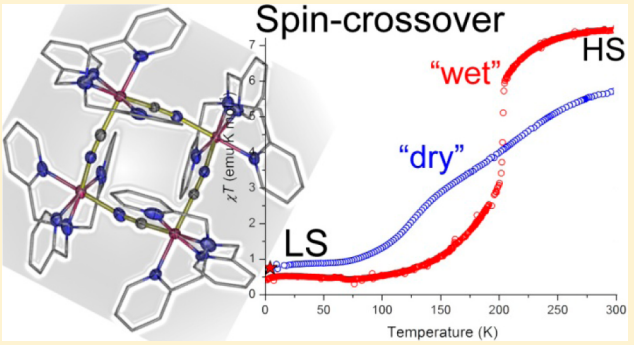

INTRODUCTION

Spin crossover (SCO) is a magnetic property of molecular and extended solids that can be observed for some compounds of d^4–d^7 transition metal ions.[1] These ions can adopt electron configurations with different numbers of unpaired electrons; hence their compounds can undergo SCO between a low-spin (LS) and a high-spin (HS) state under external stimuli such as a change in temperature, pressure, or light irradiation. Cooperativity of intermolecular interactions may lead to bistability in SCO materials, which is especially appealing for potential applications in data storage. The quest for materials useful for such applications explains the extensive research carried out on SCO complexes over the last half a century. These research efforts have been dominated by studies of Fe(II) complexes, which account for ∼90% of known SCO compounds.[2] The majority of these complexes have been mononuclear; in contrast, studies of polynuclear SCO complexes, particularly those with more than two metal centers, are still rare.[3]

The cyanide ion represents an excellent bridging ligand for the assembly of polynuclear transition metal complexes.[4] When coordinated through the carbon end, the CN^- behaves as a strong-field ligand that usually fosters a LS configuration of a metal ion. The CN^- ion coordinated through the nitrogen end acts as an intermediate-field ligand, and Fe(II) ions with such CN^- ligands might show SCO, provided that appropriate coligands are employed, such as N-imine donors. Two common types of CN-bridged SCO polynuclear complexes are pentanuclear trigonal-pyramidal clusters, which have been recently reviewed,[5] and tetranuclear clusters {[(L)M-(CN)$_2$]$_2$[Fe(L′)]$_2$}X$_4$ (M = Fe, Ru; X = counterion). In the latter category, L and L′ represent either a tetradentate ligand or a pair of bidentate ligands, often referred to as capping or blocking ligands because they prevent the formation of extended CN-bridged structures in the solid state. Crystal structures of such complexes usually contain interstitial solvent molecules, which we omit from formulas in this introduction for the sake of simplicity.

The first examples of tetranuclear CN-bridged squares, {[(bpy)$_2$M(CN)$_2$]$_2$[Fe(bpy)$_2$]$_2$}(PF$_6$)$_4$ (M = Fe, Ru; bpy = 2,2′-bipyridine), were reported by Oshio et al.[6] In these compounds, two Fe(II) sites are in the environment of six N atoms, {N$_6$}, two from the bridging CN^- ligands and four from the chelating bpy ligands. These sites showed LS state at all temperatures, indicating that the ligand field was too strong for the occurrence of SCO. Subsequently, the same group

Received: September 13, 2014
Published: December 2, 2014

   dx.doi.org/10.1021/ic502215h | Inorg. Chem. 2014, 53, 13070–13077

demonstrated that the replacement of the pair of bpy ligands with a tetradentate tris(2-pyridylmethyl)amine (tpma) or with two bidentate bipyrimidines (bpym) weakened the ligand field at $\{N_6\}$-coordinated Fe(II) ions sufficiently to result in temperature-induced SCO in the tetranuclear clusters $\{[(bpy)_2Fe(CN)_2]_2[Fe(tpma)]_2\}(PF_6)_4$[7] and $\{[(bpy)_2Fe(CN)_2]_2[Fe(bpym)_2]_2\}(PF_6)_4$.[8] Similar SCO complexes were reported by Real and co-workers, who used 1,10-phenanthroline (phen) instead of bpy to obtain $\{[(phen)_2Fe(CN)_2]_2[Fe(tpma)]_2\}(PF_6)_4$.[9] An interesting tetranuclear complex reported recently by Kepert et al. had a bis-bidentate 2,3-bis[{3-(pyridin-2-yl)-1*H*-pyrazol-1-yl}methyl]quinoxaline ligand bridging two Fe(II) ions along each edge of the square cluster and additionally coordinating to each of the two Fe(II) ions through a 3-(pyridin-2-yl)-1*H*-pyrazol-1-yl arm. This complex represents a hybrid architecture that displays features of both CN-bridged and grid-like assemblies. Nevertheless, the $\{N_6\}$-coordinated Fe(II) sites are in the HS state at all temperatures.[10]

Synthesis of the SCO heteroleptic tetranuclear complexes $\{[(L)Fe(CN)_2]_2[Fe(L')]_2\}X_4$ ($L \neq L'$) listed above required the separate preparation of the $[FeL(CN)_2]$ and $[FeL']^{2+}$ building blocks. Ligand redistribution side reactions may occur during such synthesis and limit the yield of the desired tetranuclear complex. This synthetic disadvantage is eliminated in the synthesis of homoleptic complexes ($L = L'$), which can be performed directly by reacting $\{FeL\}^{2+}$ (or $\{FeL_2\}^{2+}$) fragments with CN^- ligands. Unfortunately, as mentioned above, such a reaction using $[Fe(bpy)_2]^{2+}$ led to a complex that did not exhibit SCO.[6a] We reasoned that the use of tpma as a sole capping ligand could lead to a homoleptically capped SCO complex. Indeed, herein we report the synthesis, crystal structure, and magnetic properties of tetranuclear, CN-bridged complexes $\{[(tpma)Fe(\mu\text{-}CN)_2]_2[Fe(tpma)]_2\}X_4$, where X = ClO_4^- or BF_4^-, both of which exhibit gradual temperature-induced SCO. The solvent-dependent SCO behavior of these complexes demonstrates the importance of the structural order for the abruptness of the SCO transition. We also compare their SCO properties to those of other complexes from the $\{[(L)Fe(CN)_2]_2[Fe(L')]_2\}X_4$ series.

MATERIALS AND METHODS

Synthesis. All reactions were performed in an inert N_2 atmosphere using standard Schlenk techniques. All reagents were purchased from Aldrich and used as received. Tris(2-pyridylmethyl)amine (tpma) was prepared according to the published procedure.[11] Anhydrous commercial solvents were additionally purified by passing through a double-stage drying/purification system (Glass Contour Inc.). Elemental analyses were performed by Atlantic Microlab, Inc., Norcross, GA, USA.

Warning! *Metal perchlorate salts used in this study are potentially explosive and should only be used on a small scale. Appropriate protective measures should always be taken when handling these compounds. Tetrabutylammonium cyanide, $(Bu_4N)CN$, is poisonous and should be handled with extreme precautions.*

$\{[Fe(tpma)(\mu\text{-}CN)]_4\}(ClO_4)_4$ (1a). To a mixture of $Fe(ClO_4)_2\cdot 6H_2O$ (0.168 g, 0.46 mmol) and tpma (0.134 g, 0.46 mmol) was added 4 mL of MeOH. The resulting clear-yellow solution was added dropwise with stirring to a solution of $(Bu_4N)CN$ (0.124 g, 0.46 mmol) in 4 mL of MeOH. The solution quickly turned dark red, followed by precipitation of an orange solid. After the addition was complete, the mixture was stirred for 20 min and left undisturbed for 30 min. The orange solid was recovered by filtration and dried under vacuum. Yield = 0.118 g (55%). Elem. analysis: calcd (found) for $Fe_4Cl_4O_{18}N_{20}C_{76}H_{76}$ (**1a**·$2H_2O$), %: C, 47.48 (47.44); H, 3.98 (4.13); N, 14.57 (14.28). IR, $\nu(C{\equiv}N)$, cm^{-1}: 2081, 2072. X-ray quality single crystals of **1a** were obtained by vapor diffusion of Et_2O into the solution of **1a** in MeCN.

$\{[Fe(tpma)(\mu\text{-}CN)]_4\}(BF_4)_4$ (1b). Complex **1b** was prepared in a manner similar to that described for **1a**, using $Fe(BF_4)_2\cdot 6H_2O$ (0.206 g, 0.610 mmol), tpma (0.177 g, 0.610 mmol), and $(Bu_4N)CN$ (0.164 g, 0.610 mmol) as starting materials. Yield = 0.144 g (51%). Elem. analysis: calcd (found) for $Fe_4F_{16}O_5N_{20}C_{76}B_4H_{82}$ (**1b**·$5H_2O$), %: C, 47.39 (47.45); H, 4.29 (4.13); N, 14.54 (14.50). IR, $\nu(C{\equiv}N)$, cm^{-1}: 2081, 2072. X-ray quality single crystals of **1b** were obtained by vapor diffusion of Et_2O into the solution of **1b** in MeCN.

Physical Measurements. The IR spectra were recorded on a PerkinElmer FT-IR spectrometer (Spectrum 100) in the 4000−600 cm^{-1} range, using a universal ATR accessory. Thermogravimetric analyses (TGA) were performed under a continuous flow of Ar gas, using a TGA Q50 thermogravimetric analyzer (TA Instruments). Cyclic voltammograms (CV) were recorded on a CH Instruments 600D electrochemical analyzer at the sweep rate of 0.100 V/s, with 0.100 M $(Bu_4N)PF_6$ in MeCN electrolyte solution, Pt working electrode, and Ag^+(0.01 M $AgNO_3$)/Ag reference electrode.

Mössbauer Spectroscopy. ^{57}Fe Mössbauer spectra of **1a** and **1b** were collected on a constant acceleration instrument at various temperatures in zero applied magnetic field. Measurements were conducted on polycrystalline samples that were either kept under the MeOH mother liquor or dried before the measurements. The dried samples were prepared by placing the crystalline solids in Mössbauer cups in open air and closing them with Teflon lids; these samples were then stored under ambient conditions. For Mössbauer analysis, the dried samples were cooled fast by immersion into liquid N_2. They were placed in the cryostat at 77 K and then warmed up from 77 K to the desired temperature (90−300 K) at rate of ∼2−3 K/min. The samples under solvent were prepared in a nitrogen glovebox by transferring the crystalline solids and MeOH mother liquor into Mössbauer cups. The samples were then removed from the glovebox and immediately frozen in liquid N_2, where they were then stored. For Mössbauer analysis at 4.2 K, the samples under MeOH were placed in the cryostat at 77 K and were cooled to 4.2 K within seconds. Spectral simulations were generated using WMOSS (WEB Research, Edina, MN). Isomer shifts are reported relative to Fe metal foil at room temperature.

Magnetic Measurements. Magnetic measurements were carried out on polycrystalline samples that were either kept under the MeOH mother liquor or dried before the measurements. The samples that were covered with solvent were contained in a sealed NMR tube, while the dried samples were placed into a tightly closed gelatin capsule. The measurements were performed with a superconducting quantum interference device (SQUID) magnetometer (Quantum Design MPMS-XL). DC susceptibility was measured in an applied field of 0.1 T in the 1.8−300 K temperature range, with the heating/cooling rate of ∼2 K/min. The data were corrected for the diamagnetic contribution from the sample holder and for the intrinsic diamagnetism using tabulated constants.[12] All dried samples contained residual interstitial water molecules, as indicated by elemental analysis. Consequently, the mass of each such sample was corrected by measuring the content of interstitial solvent by TGA immediately after magnetic measurements. The mass of the samples stored under MeOH was obtained by measuring the mass of the entire sample that included the solid and the mother liquor, followed by the weighing of the dry sample that was recovered from the NMR tube after the magnetic measurements had been completed. The difference provided the mass of mother liquor, the diamagnetic correction for which was approximated to be equal to the contribution of the pure MeOH solvent.[12]

X-ray Crystallography. Single-crystal X-ray diffraction experiments on **1b** were performed on a Bruker APEX-II CCD X-ray diffractometer equipped with a graphite-monochromated Mo Kα source (λ = 0.71073 Å). A selected single crystal was suspended in Paratone-N oil (Hampton Research) and mounted on a cryoloop which was placed in an N_2 cold stream and cooled down to the desired data collection temperature. The data sets were recorded as ω scans at

dx.doi.org/10.1021/ic502215h | *Inorg. Chem.* 2014, 53, 13070−13077

Table 1. Data Collection and Structure Refinement Parameters for Complex 1b at 100 and 210 K

	$Fe_4F_{16}ON_{21}C_{78}B_4H_{75}$ (**1b**·CH_3CN·H_2O)	$Fe_4F_{16}ON_{20.75}C_{77.5}B_4H_{73.5}$ (**1b**·0.75CH_3CN·H_2O)
temperature, K	100(2)	210(2)
CCDC number	918599	918600
formula weight	1893.23	1882.21
space group	*C*2/*c*	*C*2/*c*
a (Å)	36.482(3)	36.995(5)
b (Å)	27.585(2)	27.796(4)
c (Å)	25.201(3)	25.479(6)
β (deg)	133.061(1)	133.253(1)
V (Å^3)	18530(3)	19083(6)
Z	8	8
crystal color	red	red
crystal size (mm^3)	0.59 × 0.12 × 0.10	0.65 × 0.18 × 0.14
d_{calc} (g cm^{-3})	1.357	1.310
μ (mm^{-1})	0.699	0.679
λ (Å)	0.71073	0.71073
$2\theta_{max}$ (deg)	26.37	26.37
total reflections	73254	74204
R_{int}	0.0431	0.0409
unique reflections	15042	19393
parameters refined	1154	1173
restraints used	32	105
R_1, wR_2 [$I > 2\sigma(I)$][a]	0.076, 0.228	0.092, 0.279
R_1, wR_2 (all data)	0.101, 0.249	0.122, 0.311
goodness of fit[b]	1.061	1.045
diff peak/hole (e Å^{-3})	0.97, −0.73	1.19, −0.80

[a] $R_1 = \sum||F_0| - |F_c||/\sum|F_0|$; $wR_2 = [\sum[w(F_0^2 - F_c^2)^2]/\sum[w(F_0^2)^2]]^{1/2}$. [b] Goodness-of-fit = $[\sum[w(F_0^2 - F_c^2)^2]/(N_{obs} - N_{params})]^{1/2}$, based on all data.

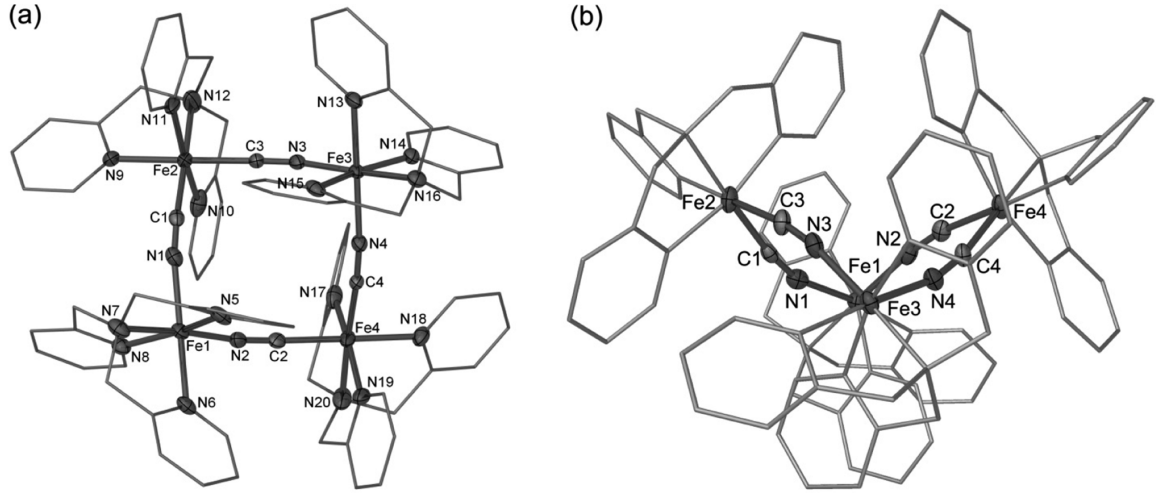

Figure 1. Two views of the molecular structure of the tetranuclear cation $\{[Fe(tpma)(\mu\text{-}CN)]_4\}^{4+}$ in **1b**. The H atoms have been omitted for clarity. Thermal ellipsoids are depicted at 50% probability level.

0.3° stepwidth and integrated with the Bruker SAINT software.[13] A multiscan adsorption correction was applied based on fitting a function to the empirical transmission surface as sampled by multiple equivalent measurements (SADABS).[14] The space group determination was performed with XPREP,[15] and the crystal structure solution and refinement were carried out using the SHELX-2013 program suite.[16] The final refinement was performed with anisotropic atomic displacement parameters for all non-hydrogen atoms, with the exception of some strongly disordered counteranions or interstitial solvent molecules, which were refined isotropically. All H atoms were placed in calculated positions and refined in the riding model. A summary of pertinent information relating to data collection and structure refinement of **1b** is provided in Table 1. The X-ray data collection was attempted for **1a** as well, but severe disorder of the counteranions and interstitial solvent molecules prevented us from obtaining a reliable refinement of the structure.

RESULTS

Synthesis. The use of only one capping ligand, namely tpma, allowed the assembly of the Fe(II) tetranuclear complexes, $\{[Fe(tpma)(\mu\text{-}CN)]_4\}X_4$ (X = ClO_4^- or BF_4^-) by addition of the bridging CN^- ligands to the preformed $[Fe(tpma)]^{2+}$ building block. It appears that the reaction proceeds via the initial formation of $[Fe(tpma)_2(CN)_2]$, as can be inferred from the change in the color of the Fe(II) precursor solution from yellow to dark red in the course of the addition of the CN-containing solution. After sufficient concentration of

dx.doi.org/10.1021/ic502215h | Inorg. Chem. 2014, 53, 13070−13077

these species has accumulated, precipitation of the tetranuclear clusters **1a** and **1b** ensues via the self-assembly of the $[Fe(tpma)]^{2+}$ and $[Fe(tpma)_2(CN)_2]$ building blocks. This notion is additionally supported by the observation that the precipitation of the tetranuclear product begins shortly after one-half of the stoichiometric amount of $(Bu_4N)CN$ has been added. As discussed, such a reaction pathway is also confirmed by the magnetic properties of **1a** and **1b**. IR spectra of the complexes revealed two C≡N stretches at 2072 and 2081 cm^{-1} (Supporting Information, Figure S1), which are typical of bridging CN^- ligands in the Fe(II)−C≡N−Fe(II) unit.[4] The complexes have been synthesized in methanol and recrystallized from CH_3CN/Et_2O. The compounds are easily oxidized by air in solution but remain stable when exposed to air for days in solid form, although moist air was observed to accelerate deterioration of samples. Upon exposure to air, the solid complexes readily exchange interstitial solvent for water, as shown by the elemental analyses. Thermogravimetric analysis performed under Ar atmosphere revealed that complexes **1a** and **1b** gradually lose interstitial solvent upon heating to ∼150 °C (Supporting Information, Figure S2). While **1b** decomposes above 300 °C, **1a** decomposes abruptly at ∼180 °C, which is explained by the explosive nature of dry perchlorate salts.

Crystal Structure. The crystal structure of **1b** features a CN-bridged tetranuclear $\{[Fe(tpma)(\mu\text{-}CN)]_4\}^{4+}$ cation (Figure 1a) in which the $[Fe_4(\mu\text{-}CN)_4]$ core has a butterfly-like geometry (Figure 1b) that is significantly different from the nearly square geometry of the core of previously reported complexes with other capping ligands.[6−10] Each Fe corner of the cluster is capped by a tpma ligand. The average Fe−Z bond lengths (Z = N or C) are listed in Table 2. The table also

Table 2. Fe−Z Bond Lengths and the Total Deviation from the Ideal Octahedral Angles (∑) around the Fe Sites in the Crystal Structure of 1b (Z = N, C)[a]

	$d(Fe-Z)_{av}$ (Å)		∑(Z−Fe−Z) (deg)	
atom	100 K	210 K	100 K	210 K
Fe1	2.022(4)	1.984(6)	68.3	68.8
Fe2	*1.962(5)*	*2.123(6)*	49.0	73.7
Fe3	1.967(4)	1.958(6)	54.8	46.8
Fe4	*1.974(5)*	*2.076(6)*	69.9	79.0

[a]The sites that undergo SCO are highlighted in italics.

contains the value of parameter ∑, which is defined as the sum of deviations of twelve Z−Fe−Z angles of each Fe site from 90°, the ideal octahedral angle. The main structural features of the tetranuclear cation in **1a** are similar to those observed in **1b**, but the strong disorder of the ClO_4^- counterions and interstitial solvent molecules precluded a reliable crystal structure refinement.

As shown by the crystal structure determination of **1b** at two temperatures, 100 and 210 K, the average Fe−Z bond lengths at two of the Fe centers, Fe(2) and Fe(4), increase at the higher temperature. The ∑ parameter increases from 49.0° at 100 K to 73.7° at 210 K for Fe(2) and from 69.9° at 100 K to 79.0° at 210 K for Fe(4), lending support to the idea that these two sites undergo SCO in the 100−210 K temperature interval. The average Fe−Z bond lengths and ∑ parameters for the sites Fe(1) and Fe(3) exhibit much smaller changes, suggesting that these ions retain their LS state.

An examination of the crystal packing in **1b** reveals that the tetranuclear cations are organized in layers parallel to the *ac* plane. As can be seen from Figure 2, the interactions between the molecules of adjacent layers are weak, mainly due to the

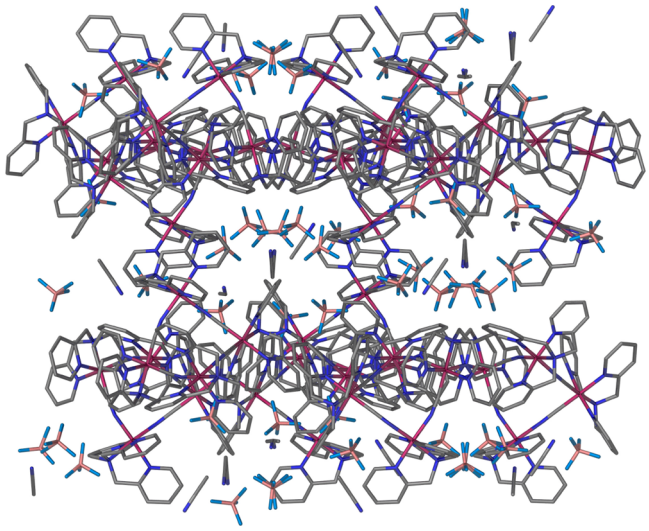

Figure 2. Crystal packing of **1b**. The H atoms have been omitted for clarity. Color scheme: Fe = red, *N* = blue, C = gray, B = pink, *F* = light-blue.

large number of the BF_4^- anions and solvent molecules located in the interlayer space. The interactions within the layers are mainly of van der Waals type, with scarce weak $\pi-\pi$ and $\sigma-\pi$ contacts between the pyridyl ring of tpma ligands.

Magnetic Properties. Magnetic susceptibility was measured on powder samples of **1a** and **1b**, as well as on samples covered with MeOH mother liquor. These samples will be referred to as "dry" and "wet", respectively, in the following discussion. As the temperature is lowered, the χT curves for both wet and dry samples show a gradual decrease consistent with the temperature-induced SCO (Figure 3). The curves obtained upon warming coincided with those recorded upon cooling. The χT values for wet samples approach a plateau of ∼7.5 emu K mol^{-1} at 300 K, consistent with the presence of two HS Fe(II) ions in each cluster. (Typical room temperature χT values for HS Fe(II) and LS Fe(II) ions are in the range of 3.3−3.8 emu K mol^{-1} and 0, respectively.[3b]) The other two Fe(II) centers remain in the LS state, in agreement with the mechanism proposed for the formation of complexes **1a** and **1b**, which leads to the two of the Fe(II) sites having the "LS" N_4C_2 coordination environment and the other two having the "HS" N_6 coordination. The coordination assignment is also confirmed by Mössbauer spectroscopy (see below).

The comparison of the χT vs T curves of wet samples **1a** and **1b** shows that for the former compound the SCO is more abrupt and nearly complete, as its χT value approaches a plateau of ∼0.5 emu K mol^{-1} below 100 K. In contrast, the χT value of wet sample **1b** reaches a plateau of ∼1.2 emu K mol^{-1} below 70 K, indicating that a significant fraction of the N_6-coordinated Fe(II) ions remains in the HS state even at low temperatures. The behavior of the dry samples is drastically different. The SCO is much more gradual and incomplete both on the high-temperature and the low-temperature sides. The residual low-temperature fraction of the HS ions in the dry sample is higher than that in the wet sample for both **1a** and **1b**. For comparison to the Mössbauer data discussed below, we also plot in Figure 3 the HS fraction for two N_6-coordinated

dx.doi.org/10.1021/ic502215h | *Inorg. Chem.* 2014, 53, 13070−13077

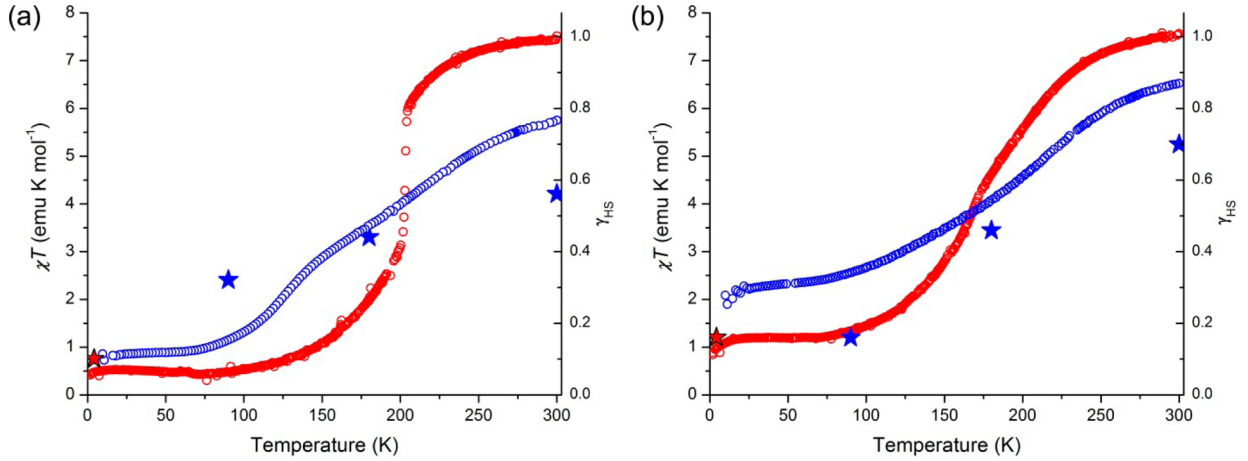

Figure 3. Temperature dependence of χT and the calculated HS fraction of two N_6-coordinated Fe(II) sites, γ_{HS}, for the wet (red curves) and dry (blue curves) samples of **1a** (a) and **1b** (b). The red and blue stars indicate the HS fraction of the N_6-coordinated Fe(II) sites obtained from Mössbauer spectroscopy studies on wet and dry samples, respectively (see Table 3).

Fe(II) sites, calculated as $\gamma_{HS} = (([Fe^{HS}])/([Fe^{HS}] + [Fe^{LS}]))$ assuming that $\chi T(Fe^{HS}) \approx 3.75(3)$ emu K mol^{-1} and $\chi T(Fe^{LS}) \approx 0$ emu K mol^{-1}. The former value was taken equal to one-half of the χT value observed for the wet sample of **1a** at 300 K.

Mössbauer Spectroscopy. We have collected ^{57}Fe Mössbauer spectra for **1a** and **1b** at various temperatures from 4.2 to 300 K in zero applied magnetic field. Analysis of the spectra provides insight into which of the four Fe(II) ions present in the molecular tetranuclear complexes undergo SCO.

The 90 K Mössbauer spectrum of dry **1a** (Figure 4a, A) shows three quadrupole doublets. Two of these doublets have

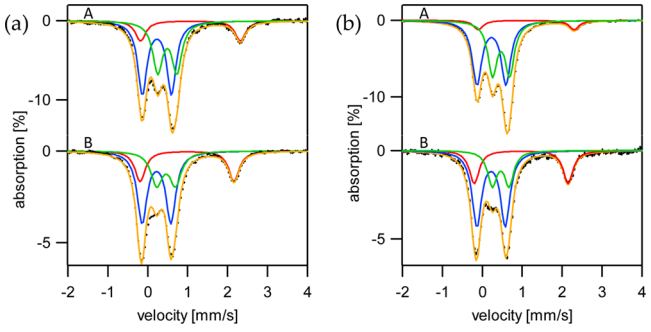

Figure 4. Mössbauer spectra recorded on dry samples of **1a** (a) and **1b** (b) at 90 K (A) and 180 K (B). The blue line represents the simulation of the contribution from LS Fe(II) ions with N_4C_2 coordination. Contributions of the LS and HS Fe(II) ions with N_6 coordination are shown in green and red, respectively. The sum of all three contributions yields the overall simulation of each spectrum shown in orange.

parameters characteristic of LS Fe(II), namely isomer shift/quadrupole splitting $\delta/\Delta E_Q = 0.23/0.72$ mm s^{-1} and 0.49/0.48 mm s^{-1}, respectively, and represent ~50% and ~35% of all Fe ions present in the sample, respectively (Table 3). The third doublet has Mössbauer parameters characteristic of HS Fe(II) ($\delta/\Delta E_Q = 1.06/2.50$ mm/s) and represents ~15% of the Fe ions in the sample. The spectrum obtained for **1a** at 180 K (Figure 4a, B) shows an increase in the amount of HS Fe(II) in the sample and a decrease in the amount of one of the two LS Fe(II) species, specifically the one that has higher isomer shift (i.e., $\delta = 0.45$ mm s^{-1} at 180 K). The LS Fe(II) ions with lower isomer shift (i.e., $\delta = 0.22$ mm s^{-1} at 180 K) continue to represent 50% of Fe in the sample (which corresponds to two Fe ions/cluster) at 180 K. We associate the low isomer shift LS Fe(II) ions with the Fe sites that coordinate two bridging CN^- ligands through the C atoms. As mentioned above, the CN^- creates a strong ligand field when coordinated through the C end; consequently, these two Fe ions are unlikely to undergo SCO, which is indeed what our Mössbauer studies showed. The LS Fe(II) ions that have higher isomer shift coordinate two CN^- ligands through the N-end and thus experience a weaker ligand field and undergo SCO.[17] These conclusions about the relationship between the C/N coordination of the Fe sites, their low/high isomer shift, and their in/ability to undergo SCO is in agreement with the results we have obtained in the study of cyanide-bridged trigonal bipyramidal, pentanuclear Fe-containing clusters.[3b,e,18] A similar gradual SCO behavior at the Fe sites with N_6-coordination was also observed for **1b** (Table 3 and Figure 4b).

The χT values at 90, 180, and 300 K for dry **1a** are 1.1, 3.5, and 5.7 emu K mol^{-1}, respectively. Thus, at 90 K, the HS fraction of N_6-coordinated Fe(II) is 0.15, significantly smaller than the value of 0.32 determined by Mössbauer spectroscopy at the same temperature. At 180 K, the amount of N_6-coordinated HS Fe(II) estimated from the magnetic χT value corresponds to a HS Fe(II) fraction of 0.47, while the Mössbauer data indicates a HS Fe(II) fraction of 0.44. At 300 K, the discrepancy grows even more as the HS Fe(II) fractions estimated from magnetometry and Mössbauer spectroscopy become 0.76 and 0.56, respectively. Hence the Mössbauer data indicates a more gradual SCO, with more HS Fe at low temperature and less HS Fe(II) at high temperature than the magnetic susceptibility data. The same dichotomy in the change in the fraction of HS Fe(II) is seen for dry **1b**, although the difference between the magnetic and Mössbauer measurements is smaller in this case. The fraction of HS Fe(II) estimated from Mössbauer spectroscopy is consistently lower than the fraction established from magnetometry (Figure 3b and Table 3).

We have considered two possible explanations for the differences in the characteristics of the SCO behavior observed by the two methods. The first could be that in the SQUID measurements the samples were loaded at room temperature and slowly cooled, while in the Mössbauer experiments they were quickly cooled within 2−3 min from room temperature to

dx.doi.org/10.1021/ic502215h | Inorg. Chem. 2014, 53, 13070−13077

Table 3. Mössbauer Parameters for the Fe Ions in the Samples of $\{[Fe(tpma)(\mu\text{-}CN)]_4\}X_4$ (1a and 1b)

compd	T (K)	δ (mm/s)	ΔE_Q (mm/s)	Fe type	%	γ_{HS} (FeN_6 only)[a]	
						Mössbauer	χT curve
1a, wet	4.2	1.09	2.51	HS-Fe(II)N_4N_2	5(1)	0.10	0.06[b]
X = ClO_4^-		0.505	0.49	LS-Fe(II)N_4N_2	45(1)		
		0.235	0.72	LS-Fe(II)N_4C_2	51(1)		
1a, dry	90	1.06(2)	2.50(2)	HS-Fe(II)N_4N_2	16(1)	0.32	0.15
X = ClO_4^-		0.49(1)	0.48(1)	LS-Fe(II)N_4N_2	35(1)		
		0.23(1)	0.72(1)	LS-Fe(II)N_4C_2	51(1)		
	180	0.98(2)	2.36(1)	HS-Fe(II)N_4N_2	22(2)	0.44	0.47
		0.45(1)	0.47(1)	LS-Fe(II)N_4N_2	28(3)		
		0.22(1)	0.72(1)	LS-Fe(II)N_4C_2	51(1)		
	300	0.82	2.15	HS-Fe(II)N_4N_2	33	0.66	0.76
		0.35	0.45	LS-Fe(II)N_4N_2	17		
		0.20	0.72	LS-Fe(II)N_4C_2	50		
1b, wet	4.2	1.10	2.50	HS-Fe(II)N_4N_2	8(1)	0.16	0.16
X = BF_4^-		0.49	0.43	LS-Fe(II)N_4N_2	43(2)		
		0.23	0.74	LS-Fe(II)N_4C_2	51(1)		
1b, dry	90	1.07(3)	2.47(7)	HS-Fe(II)N_4N_2	8(1)	0.16	0.34
X = BF_4^-		0.47(1)	0.44(1)	LS-Fe(II)N_4N_2	42(2)		
		0.23(1)	0.71(2)	LS-Fe(II)N_4C_2	52(2)		
	180	0.98(1)	2.35(1)	HS-Fe(II)N_4N_2	23(1)	0.46	0.54
		0.46(1)	0.43(1)	LS-Fe(II)N_4N_2	25(2)		
		0.22(1)	0.71(1)	LS-Fe(II)N_4C_2	51(1)		
	300	0.83	2.15	HS-Fe(II)N_4N_2	35	0.70	0.86
		0.30	0.42	LS-Fe(II)N_4N_2	15		
		0.20	0.70	LS-Fe(II)N_4C_2	50		

[a]The HS fraction of Fe(II) centers was calculated as $\gamma_{HS} = (([Fe^{HS}])/([Fe^{HS}] + [Fe^{LS}]))$, where the relative concentrations of the HS and LS fractions, $[Fe^{HS}]$ and $[Fe^{LS}]$, were taken only over the sites with the FeN_6 coordination, assuming that $\chi T(Fe^{HS}) \approx 3.75$ emu K mol^{-1} and $\chi T(Fe^{LS}) \approx 0$ emu K mol^{-1}. [b]The value of χT at 4.2 K is significantly reduced by the zero-field splitting effect. Therefore, the value of γ_{HS} at this temperature was estimated from the χT value at 50 K, taking into account that the HS → LS conversion essentially does not proceed below 70 K.

Table 4. Other Tetranuclear CN-Bridged Fe(II) Complexes that Exhibit SCO Behavior and the Parameters of Their Mössbauer Spectra

compd	T (K)	δ (mm/s)	ΔE_Q (mm/s)	Fe type	%	γ_{HS} (FeN_6 only)[a]	
						Mössbauer	χT curve
$\{[(bpy)_2Fe(CN)_2]_2[Fe(tpma)]_2\}(PF_6)_4$[7]	50	1.13	2.26	HS-Fe(II)N_4N_2	4	0.08	0.1
		0.43	0.43	LS-Fe(II)N_4N_2	44		
		0.21	0.66	LS-Fe(II)N_4C_2	52		
	160			HS-Fe(II)N_4N_2	18	0.38	
				LS-Fe(II)N_4N_2	29		
				LS-Fe(II)N_4C_2	53		
	300			HS-Fe(II)N_4N_2	21	0.49	
				LS-Fe(II)N_4N_2	22		
				LS-Fe(II)N_4C_2	56		
$\{[(bpy)_2Fe(CN)_2]_2[Fe(bpym)_2]_2\}(PF_6)_4$[8]	20	0.40	0.36	LS-Fe(II)N_4N_2	48	0	0
		0.22	0.69	LS-Fe(II)N_4C_2	52		

[a]The HS fraction of Fe(II) centers was calculated as $\gamma_{HS} = (([Fe^{HS}])/([Fe^{HS}] + [Fe^{LS}]))$, where the relative concentrations of the HS and LS fractions, $[Fe^{HS}]$ and $[Fe^{LS}]$, were taken only over the sites with the FeN_6 coordination, assuming that $\chi T(Fe^{HS}) \approx 3.75$ emu K mol^{-1} and $\chi T(Fe^{LS}) \approx 0$ emu K mol^{-1}.

77 K. This explanation was ruled out by measuring the magnetic properties of a dry sample of **1b**, which was first flash-cooled from room temperature to 77 K in ~30 s within the SQUID cavity. The χT values for this sample measured right after being quenched in the heating mode from 80 to 300 K and then in the cooling mode from 300 to 80 K (Supporting Information, Figure S3) coincided with the χT values of the dry sample that was slowly cooled from 300 K at 2 K/min.

We attribute the difference in the character of SCO to differences in the exact solvent content of the samples examined by magnetic susceptibility and Mössbauer spectroscopy. To check this possibility, we examined by these two physical methods samples of **1a** and **1b** that were kept under solvent at all times and observed smaller differences in the γ_{HS} values determined for wet **1a** and **1b** at 4.2 K (see Figure 3b, Supporting Information, Figure S4, and Table 3).

Electrochemical Properties. The two distinctly different coordination modes for the Fe(II) centers were also evidenced in the cyclic voltammetry measurements that revealed two successive quasi-reversible two-electron redox processes with

dx.doi.org/10.1021/ic502215h | Inorg. Chem. 2014, 53, 13070−13077

$E_{1/2}$ = 0.55 and 1.13 V vs Ag^+(0.01 M $AgNO_3$)/Ag (Supporting Information, Figure S5). On the basis of the expected energies of the Fe 3*d* orbitals, which should be stabilized by strong-field ligands, the observed redox waves are assigned to the oxidation of the FeN_6 and FeN_4C_2 centers, respectively. Nevertheless, the separations between the anodic and cathodic peaks, 0.186 and 0.132 V, respectively, are much larger than the value of 0.0296 V that would be expected for a reversible two-electron process. This observation suggests a weak electronic coupling between the Fe centers in the CN-bridged cluster core.

DISCUSSION

The complexes $\{[(L)Fe(CN)_2]_2[Fe(L)]_2\}X_4$ (**1a** and **1b**) are the first homoleptically-capped tetranuclear Fe(II) clusters to exhibit temperature-driven SCO; the transition is gradual and occurs between 80 K and room temperature. The Fe(II) ions in the previously reported homoleptically capped complex $\{[(bpy)_2Fe(CN)_2]_2[Fe(bpy)_2]_2\}(PF_6)_4$ existed in the LS state up to room temperature.[6a] On the other hand, the non-homoleptically capped tetranuclear complexes $\{[(bpy)_2Fe(CN)_2]_2[Fe(tpma)]_2\}(PF_6)_4$,[7] $\{[(bpy)_2Fe(CN)_2]_2[Fe(bpym)_2]_2\}(PF_6)_4$,[8] and $\{[(phen)_2Fe(CN)_2]_2[Fe(tpma)]_2\}(PF_6)_4$[9] exhibit SCO. As one would expect, the LS ↔ HS interconversion in **1a** and **1b** and in the previously reported $\{[(L)Fe(CN)_2]_2[Fe(L')]_2\}X_4$ complexes (Table 4) occurs at two of the four Fe(II) ions, those with the FeN_6 coordination environment.

The counteranion X^- and type and amount of solvent in **1a** and **1b** exert an influence on the character of the SCO in these compounds. The influence of the counterion is relatively small, which may be due to the facts that the packing of the tetranuclear cations is relatively loose (Figure 2) and the intermolecular interactions are weak. The loose nature of crystal packing in **1a** and **1b** could be conjectured from significant disorder of the X^- counteranions and interstitial solvent molecules: the disorder in the structure with $X^- = BF_4^-$ resulted in a rather high *R*-factor (~8%) and the disorder in the structure with $X^- = ClO_4^-$ was so severe that we could not attain a well-converged refinement ($R \sim 20\%$). Such poor values of the *R*-factor are not unusual for these systems.[9]

The relative amount of the solvent may cause changes in the crystallinity of the samples, which in turn affect more strongly the SCO behavior. The samples kept wet (under mother liquor) would better maintain their crystallinity and show a nearly complete conversion of two of the Fe(II) centers to the HS state at 300 K (Figure 3). On the other hand, dry samples with poorer crystallinity would show a more gradual and incomplete SCO.[19] The effect appears to be much more significant in the case of **1b**. Both magnetic measurements on wet sample of **1b** and crystal structure determination at 110 K indicate that this complex exists in nearly pure LS state at low temperature. The dry sample of **1b**, however, contains a much larger fraction of the HS Fe(II) centers at around 100 K (Table 3).

We also note that the SCO observed for $\{[(bpy)_2Fe(CN)_2]_2[Fe(tpma)]_2\}(PF_6)_4$,[7] $\{[(bpy)_2Fe(CN)_2]_2[Fe(bpym)_2]_2\}(PF_6)_4$,[8] and $\{[(phen)_2Fe(CN)_2]_2[Fe(tpma)]_2\}(PF_6)_4$[9] is also gradual and incomplete at 300 K, which may suggest that crystal packing of the tetranuclear complexes is in general loose and not conducive of the cooperative SCO behavior that would lead to a more abrupt spin transition. Increasing the ability of the capping ligands to participate in intermolecular interactions, e.g., $\pi-\pi$ interactions or hydrogen bonding, may be a strategy to better pack polynuclear SCO cations and counteranions in the crystal lattice, to promote stronger elastic interactions between the SCO molecules and to make the spin transition in such complexes more cooperative/abrupt.

CONCLUSIONS

The $\{[(tpma)Fe(\mu\text{-}CN)]_4\}X_4$ ($X = ClO_4^-$, **1a**; BF_4^-, **1b**) complexes are the first example of homoleptically-capped tetranuclear CN-bridged Fe(II) complexes that exhibit SCO. While it was typically observed in previous studies that dry samples of SCO Fe(II) compounds show more abrupt transitions than solvent-covered ones, the opposite is the case for complexes **1a** and **1b**, an effect that may relate to the crystallinity of the samples. This finding emphasizes the importance of studying the magnetic properties of such materials both under mother liquor and in the dry form.

ASSOCIATED CONTENT

Supporting Information

IR spectra, TGA analyses, and cyclic voltammograms of **1a** and **1b**, additional magnetic plots and Mössbauer spectra, and CIF files. This material is available free of charge via the Internet at http://pubs.acs.org.

AUTHOR INFORMATION

Corresponding Authors

*E-mail: achim@cmu.edu.

*E-mail: shatruk@chem.fsu.edu.

Present Address

[⊥]Department of Chemistry, University of California at Davis, Davis, California 95616, United States.

Author Contributions

[‖]O.H. and P.W.D. contributed equally to the work reported in the paper.

Notes

The authors declare no competing financial interest.

ACKNOWLEDGMENTS

This work was supported in part by the U.S. National Science Foundation (award CHE-0911109 to M.S.).

REFERENCES

(1) *Spin-Crossover Materials: Properties and Applications*; Halcrow, M. A., Ed.; John Wiley & Sons Ltd.: 2013.

(2) Gütlich, P.; Goodwin, H. A. *Top. Curr. Chem.* **2004**, *233*, 1−47.

(3) (a) Breuning, E.; Ruben, M.; Lehn, J. M.; Renz, F.; García, Y.; Ksenofontov, V.; Gütlich, P.; Wegelius, E.; Rissanen, K. *Angew. Chem., Int. Ed.* **2000**, *39*, 2504−2507. (b) Shatruk, M.; Dragulescu-Andrasi, A.; Chambers, K. E.; Stoian, S. A.; Bominaar, E. L.; Achim, C.; Dunbar, K. R. *J. Am. Chem. Soc.* **2007**, *129*, 6104−6116. (c) Herchel, R.; Boča, R.; Gembický, M.; Kožíšek, J.; Renz, F. *Inorg. Chem.* **2004**, *43*, 4103−4105. (d) Berlinguette, C. P.; Dunbar, K. R. *Chem. Commun.* **2005**, 2451−2453. (e) Hilfiger, M. G.; Chen, M.; Brinzari, T. V.; Nocera, T. M.; Shatruk, M.; Petasis, D. T.; Musfeldt, J. L.; Achim, C.; Dunbar, K. R. *Angew. Chem., Int. Ed.* **2010**, *49*, 1410−1413. (f) Matsumoto, T.; Newton, G. N.; Shiga, T.; Hayami, S.; Matsui, Y.; Okamoto, H.; Kumai, R.; Murakami, Y.; Oshio, H. *Nature Commun.* **2014**, *5*, 3865 DOI: 10.1038/ncomms4865. (g) Steinert, M.; Schneider, B.; Dechert, S.; Demeshko, S.; Meyer, F. *Angew. Chem., Int. Ed.* **2014**, *53*, 6135−6139.

(4) Shatruk, M.; Avendano, C.; Dunbar, K. R. *Prog. Inorg. Chem.* **2009**, *56*, 155−334.

(5) Funck, K. E.; Hilfiger, M. G.; Berlinguette, C. P.; Shatruk, M.; Wernsdorfer, W.; Dunbar, K. R. *Inorg. Chem.* **2009**, *48*, 3438−3452.
(6) (a) Oshio, H.; Onodera, H.; Tamada, O.; Mizutani, H.; Hikichi, T.; Ito, T. *Chem.—Eur. J.* **2000**, *6*, 2523−2530. (b) Oshio, H.; Onodera, H.; Ito, T. *Chem.—Eur. J.* **2003**, *9*, 3946−3950.
(7) Nihei, M.; Ui, M.; Yokota, M.; Han, L.; Maeda, A.; Kishida, H.; Okamoto, H.; Oshio, H. *Angew. Chem., Int. Ed.* **2005**, *44*, 6484−6487.
(8) Nihei, M.; Ui, M.; Oshio, H. *Polyhedron* **2009**, *28*, 1718−1721.
(9) Boldog, I.; Muñoz-Lara, F. J.; Gaspar, A. B.; Muñoz, M. C.; Seredyuk, M.; Real, J. A. *Inorg. Chem.* **2009**, *48*, 3710−3719.
(10) Li, F.; Clegg, J. K.; Goux-Capes, L.; Chastanet, G.; D'Alessandro, D. M.; Létard, J. F.; Kepert, C. J. *Angew. Chem., Int. Ed.* **2011**, *50*, 2820−2823.
(11) Tyeklár, Z.; Jacobson, R. R.; Wei, N.; Murthy, N. N.; Zubieta, J.; Karlin, K. D. *J. Am. Chem. Soc.* **1993**, *115*, 2677−2689.
(12) Bain, G. A.; Berry, J. F. *J. Chem. Educ.* **2008**, *85*, 532−536.
(13) *SMART and SAINT*; Bruker AXS Inc.: Madison, WI, 2007.
(14) Sheldrick, G. M. *SADABS*; University of Göttingen: Göttingen, Germany, 1996.
(15) Sheldrick, G. M. *XPREP: Space Group Determination and Reciprocal Space Plots*; Siemens Analytical X-ray Instruments: Madison, WI, 1991.
(16) Sheldrick, G. M. *Acta Crystallogr., Sect. A* **2008**, *A64*, 112−122.
(17) Purcell, K. F.; Yeh, S. M.; Eck, J. S. *Inorg. Chem.* **1977**, *16*, 1708−1715.
(18) Berlinguette, C. P.; Dragulescu-Andrasi, A.; Sieber, A.; Güdel, H. U.; Achim, C.; Dunbar, K. R. *J. Am. Chem. Soc.* **2005**, *127*, 6766−6779.
(19) Indeed, the crystals of **1a** or **1b** taken out of mother liquor lost a distinct single-crystal diffraction pattern if kept at room temperature for a few minutes.